Jurnal Mekanikal
June 2014, No 37, 47-63

Fluid Flow Characteristic around Round-Shaped FPSO

Jaswar, Mufti Fathonah Muvariz, Siow.C.L

Department of Aeronautics, Automotive and Ocean Engineering,
Faculty of Mechanical Engineering,
Universiti Teknologi Malaysia
81310 Johor Bahru, Johor, Malaysia,

ABSTRACT

Liquefied Natural Gas (LNG) is currently representing almost 30% of the imported natural gas worldwide. In order to cover the demand of LNG, there is growing interest to unlock and monetize these reserves with LNG FPSO (Liquefied Natural Gas Floating Production Storage Offloading) facilities. Development of design concepts of the FPSO starts with a shape like a ship. Nowadays concept of FPSO is round-shaped which is given much advantage than the ship-shaped. Fluid flow around hull is one of phenomena that occur on the round-shaped FPSO during the operation. Fluid flow characteristic around round-shaped FPSO is presented by developing Computational Fluid Dynamics (CFD) code based on Reynolds Average Navier-Stokes (RANS) method. The simulation program is developed using Fortran language. Pressure distribution, axial velocity, and wave elevation around the hull are simulated using CFD code with different Froude numbers. Grids of the hull are generated using Maxsurf software before simulated. The obtained result found the critical part at stern (0.6 < X/(L/2) < 1).

Keywords: *FPSO LNG; RANS; CFD*

1. INTRODUCTION

Liquefied Natural Gas is currently representing almost 30% of the imported natural gas worldwide. LNG is the clean energy alternative compared to oil and coal. This is especially important in view of rising concerns about environmental pollution and nuclear power plant hazards.In many cases, development of offshore gas exploration industry, particularly are shifted into deep water. Correspondingly with the increase in oil and gas exploration in deep ocean waters, there is growing interest to unlock and monetize these reserves with a LNG FPSO (Liquefied Natural Gas Floating Production Storage Offloading) facility capable of liquefying and storing natural gas. The LNG FPSO is functioned to receive and process gas from the seabed and save the LNG into Cargo Containment System (CCS) tank before the LNG transferred to the LNG Carrier to be distributed to the market or destination. Development of the LNG FPSO facilities is technically complex and challenging.LNG FPSO effectively to be used if the reservoir away from the inland terminals, given the fact that it can perform as a result of production and offload the gas product to the shuttle tanker. It is also effective to access the restrict reservoir at sea, may not be able to connect through the service pipe as some restrictions. FPSO improves operations in the sea because it does not require the need for transportation to the onshore base terminal facilities for processing other than just to offload to the shuttle tanker.Depth water operation will cause the construction of fix structures to remain ineffective. In addition, future costs for depleting structure remains inadequate.

Development of design concepts of the FPSO start with a shape like a ship. The FPSO is designed to accommodate the construction of the module production process to be the product oil. The next generation of the FPSO provides the industry a new and exciting area of creativity and optimization. The new concept design of the FPSO is currently a round-shaped being developed by Sevan Marine [22] and SSP Offshore [24]. Round-shaped FPSO has the advantage on motions due to same shape from all directions with little to no yaw excitation, more efficient storage shape and the smaller bending loads, smaller sloshing forces, allows for larger freeboard, simple block construction and repeatable fabrication [1]. Another new design concept of the

*Corresponding author: jaswar@fkm.utm.my

FPSO is studied by Wang, Zhang, and Liu which has proposed a non-ship-shape FPSO called inverted fillet quadrangular frustum pyramid-shaped FPSO (IQFP) [32].

Environmental loads generally occur in the structure at time of the FPSO operation conditions. These environmental loads are classified into three types which are wind, wave and current load. Wind load exerts a force on the part of the structure exposed to the air. Wave load and current load exerts force on the part of the structure exposed to the water. These three loads will determine the external forces on structures, stability, and motion of floating structures also patterns of fluid flow around the structure.

Fluid flow around a structure can significantly alter the structure's loading characteristics. Waves and currents is a fluid that has the most impact on the structure. Influence of fluid flow generated from waves and currents on floating structure is seen in the form of motion and pressure distribution. These motions and pressure distribution that occurs in the structure depend on the characteristic of the fluid flow. Characteristic of the fluid flow is affected by several factors such as the shape of the structure, Reynolds Number and Froude number.

The study of fluid flow around the hull of round-shaped FPSO has been performed by Lamport and Josefsson, [17]. The studies show the current induced velocity fields on the leeward side of the vessel for a round-shaped versus a traditional ship-shaped FPSO. The study of fluid flow around the hull in side-by-side offloading condition has been performed by Arslan, Pettersen, and Andersson [4]. The calculations of three dimensional (3D) unsteady cross flow past a pair of ship sections in close proximity and the behaviour of the vortex-shedding around the two bluff bodies is investigated numerically by using the software FLUENT. Present study discusses an analysis of flow around a round-shaped FPSO LNG. The fluid flow characteristic around the round-shaped LNG FPSO conducted using Computational Fluid Dynamics (CFD) based on the governing Reynolds Average Navier-Stokes (RANS) equations in the Integrated CFD simulation tool [12].

2. LITERATURE REVIEW

Studies of the fluid flow on the hull of the ship have been performed by many researchers in the last decade. For the viscous flow around ship's hull field, Zhang, Zhao, and Li performed numerical simulation free surface flow around Wigley hull [34]. Numerical simulation using RANS method and SST k-w turbulence model was performed by Zhao, F., Zhang, Z. -R with a complex modern ship model DTMB 5415 [35]. Schweighofer et al [21] focuses on the applicability of different RANS methods to full-scale viscous flow computations, Alexe [3] study about the effects of dimensional and movement parameters of the ship on the pressure distributions in the surrounding sea water. Zhao, Zhu, and Zhang study the flow around Wigley and DTMB 5415 hull using RANS, and Visonneau [36] predicting the full-scale viscous flow field around a ship including the evaluation of the free surface, the wake field, the hull/propeller interaction, the resistance and the power.

Kinnas, Yu, and Vinayan [16] study the unsteady viscous flow over the bilge keels of an FPSO hull subject to roll motions. Wang, Zou, and Tian study the viscous flow field around a KVLCC2 model moving obliquely in shallow water using a general purpose computational fluid dynamics (CFD) package FLUENT [30]. Wang et al study the wake field in viscous flow and resistance prediction of a full ship-KVLCC2M by using FLUENT [31]. For coupling the 3D incompressible RANS equations with the level set method was performed by Wan, Shen, and Ma [29] with numerical simulation. In 2011, Wackers et al [28] reviewed the surface descretisation methods with different code. Wanderley et al (2012) contributed on numerical solution of the viscous flow around the ship-like bodies. Hu study the flow around high-speed ship model by using FLUENT software [33].

For the turbulence flow around a ship hull field, many researchers have been studying it. Kim[14] study the three-dimensional turbulent flow using RANS equations. In 2002, Kim, Kim, and Van Suak [15] developed an efficient and robust numerical method for turbulent flow calculation. Ciortan et al, [7] investigates free surface incompressible turbulent flow around the hull by using a numerical solution of the unsteady Navier-Stokes equations for

slightly compressible flows. Deng, Queutey, and Visonneau [11] study the simulation of two appended hull configurations using all hexahedral unstructured grids. Three-dimensional turbulent flow around a Wigley hull using slightly compressible flow formulation were performed by Ciortan, Wanderley, and Soares [9]. Lungu [18] presented a methodology for computing the 3D turbulent free-surface flow.

Ciortan, Soares, and Wanderley [6] studied the turbulent and laminar free-surface flow around ship hulls using slightly compressible flow formulation. Ahmed, Fonfach, and Soares [2] investigated the flow pattern around the DTMB 5415 hull at two speeds. In 2011, Ahmed [1] uses the Volume of Fluid method (VOF) to simulate the flow pattern around the DTMB 5415 hull at two speeds. Ciortan, Wanderley, and Soares [10] study the simulation of flow around a Wigley hull using the slightly compressible flow formulation.

Tahara et al [26] evaluates the computational fluid dynamics (CFD) as a tool for hull form design along with application of state-of-the-art technology in the flow simulations. Two Reynolds-averaged Navier-Stokes (RANS) equation solvers were employed, namely CFD Ship-Iowa version 4 and Flowpack version 2004e, for the towing and self-propulsion cases, respectively. An accurate, efficient algorithm for solving free surface flows around ship hulls using a compressive advection discretization which maintains a sharp free surface interface representation without relying on a small time step (Zwartet al. [37]).

The application of the Fluent code to the numerical simulation of the free-surface flow around a model naval ship; the DTMB 5415. Simulations were performed using both a structured hexahedral mesh and an unstructured tetrahedral mesh of lower resolution. The results show that Fluent is able to accurately simulate the total ship resistance, near-field wave shapes, and the velocity field in the propeller plane (Jones and Clarke, [13]).

Tahara et al [25] conducted research on high-speed multi hull. Multi hull which is used in that research is a catamaran hull with forward speed. In 2011, Broglia, Zaghi and Di Mascio [5] study about the simulations of the flow around a high speed vessel in both catamaran and monohull, carried out by the numerical solution of the Reynold averaged Navier–Stokes (RANS) equations.

Studies of fluid flow around the hull of round-shaped FPSO have been performed by Lamport and Josefson (2008) [1]. The studies show the current induced velocity fields on the leeward side of the vessel for a round-shaped versus a traditional ship-shaped FPSO, but study of fluid flow around the hull of round-shaped FPSO and LNG carrier during offloading conditions have not been performed yet. The study of fluid flow around the hull in side-by-side offloading condition has been performed by Arslan, Pettersen, and Andersson [4]. The calculations of three dimensional unsteady cross flow past a pair of ship sections in close proximity and the behavior of the vortex-shedding around the two bluff bodies is investigated numerically by using the software FLUENT.

Jaswar et al [12] had studied hull performance of VLCC tanker using an integrated CFD simulation in Naval Architect and Offshore (NAO) software which is developed in UTM. The Integrated CFD simulation tool using potential theory intends to upgrade student's level understanding the application of fluid dynamic to ship and offshore structure designs. The study discussed on wave resistance, pressure distribution around the hull, and wave profile. The same software also applied to study fluid flow around Round shape FPSO [38].

3. METHODOLOGY

Flowchart of the present study is shown in the Figure 1 which is started from collecting data, developing, governing equation for CFD, developing CFD code using Reynolds-Average Navier Stokes (RANS) method which in used for CFD simulation, From the RANS equation then design the code by using Fortan software, modeling the round-shaped FPSO and results and analysis. Third steps are running the simulation on RANS code by using Fortran software. The result of the simulation of the Fortran software is hull pressure, velocity and wave height. From the result, provide the fluid flow around the hull of the rounded - shape FPSO.

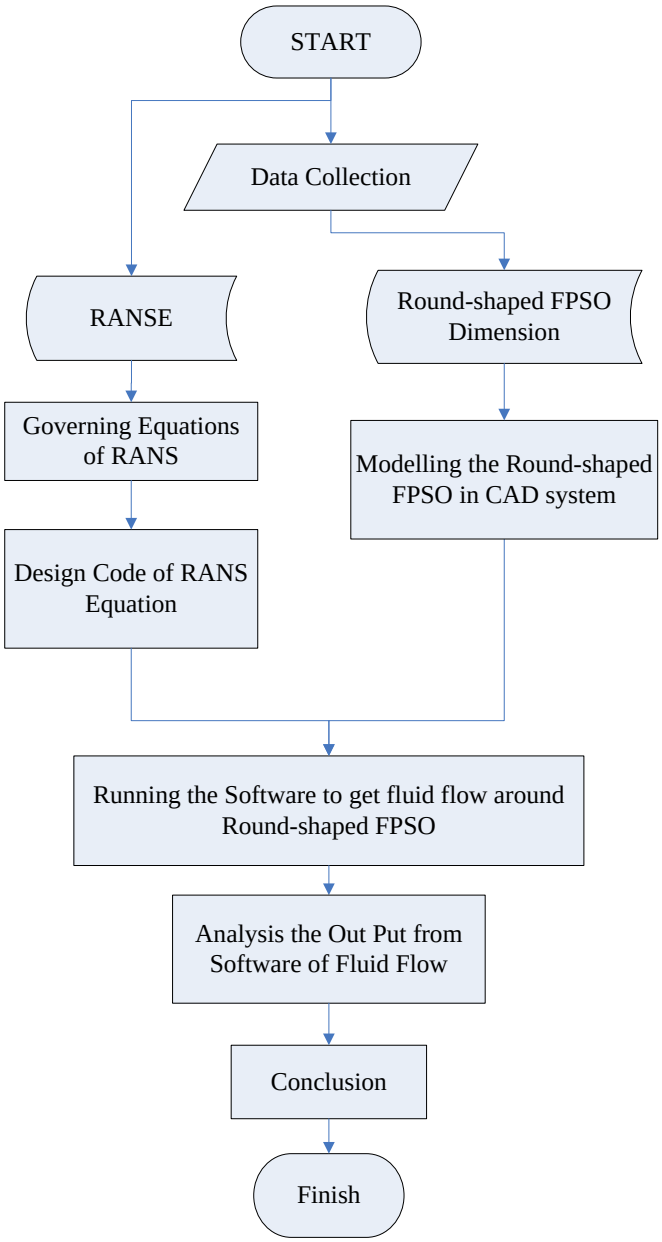

Fig. 1 Flow Chart of Present Study

4. FUNDAMENTAL THEORY

4.1 Round-shaped FPSO

According to Paik and Thayamballi [19], the first floating, production, storage and offloading vessel (FPSO), Shell's Castellon, were installed in 1977. Since the industry has seen a large and diverse suite of different FPSO solutions, from converted tankers to purpose-built barge shaped vessels. Until recently, most FPSOs had one thing in common that the design philosophy was based on classic ship-shaped vessels. While a ship has beneficial characteristics for transporting cargo from one location to another, with great maneuverability and little water resistance, it's slender and non-ax symmetrical shape presents major disadvantages when permanently moored in one location.

Such disadvantage is that ship-shape vessels must be able to align themselves with the predominantly sea state to minimize their motions and vessel stresses. The oil and gas industry mitigated this problem by developing turrets and swivels, which allowed the ship shaped vessels to weathervane into the predominant sea state. Though swivels and turrets allow ship-shaped vessels to weathervane, they are costly, have long lead times and are typically available from only few specialized designers and fabricators. Swivels and turrets also have associated maintenance requirements and potential downtime (from leaking seals, for example).

The current shape of FPSO is a rounded - shape. This shape proposes by some researcher [1], Srinivasan et al [23], Wang, Zhang, and Liu [32], Sevan Marine ASA [22], SSP [24]) which have the advantages compared to ship-shape. According to Lamport and Josefsson [17] Round-shaped has the several advantages, as follow:

a) More efficient storage shape and the smaller bending load;
b) The motions are similar from all directions with little to no yaw excitation;
c) More efficient storage shape and the smaller bending load;
d) The pie-shaped tanks in round-shaped units create smaller sloshing forces;
e) Providing additional savings in structural reinforcement;
f) Allows for larger freeboard, decreases the risk of green water on the deck; and
g) Simple block construction and repeatable fabrication.

4.2 Computational Fluid Dynamic (CFD)

There are two fundamental approaches to the design and analysis of engineering systems that involve fluid flow: experimentation and calculation. The former typically involves construction of models that are tested in wind tunnel or towing tank, while the latter involves solution of differential equations, either analytically or computationally. In the present study provide a fluid flow around round-shaped FPSO hull by using a CFD.

CFD is a branch of fluid mechanics that uses numerical methods and algorithms to solve and analyze problems that involve fluid flows. Computers are used to perform the calculations required to simulate the interaction of liquids and gases with surfaces defined by boundary conditions. With high-speed supercomputers, better solutions can be achieved. In the present sub chapter, provide a brief of computational fluid dynamic (CFD), the field of study devoted to the solution of the equations of fluid flow through the use of a computer.

4.2.1 Incompressible Potential Flow

Incompressible flow is constant density flow, i.e. ρ=constant. Visualize a fluid element of fixed mass moving along a streamline in an incompressible flow. Because its density is constant, then the volume of the fluid element is also constant. Determine $\nabla \vec{V}$ to the time rate of change of the volume of a fluid element, per unit volume. Since the volume is constant for a fluid element in incompressible flow, the equation becomes:

$$\nabla \cdot \vec{V} = 0 \qquad (1)$$

Furthermore, if the fluid element does not rotate as it moves along the streamline, i.e. if its motion is translational only, then the flow is called irrotational flow. For such flow, the velocity can be expressed as the gradient of a scalar function called the velocity potential, denoted by ∅.

$$\overline{V} = \nabla \emptyset \tag{2}$$

Combining Eq.(1) and Eq.(2),

$$\nabla \cdot \nabla \emptyset = 0$$

or,

$$\nabla^2 \emptyset = 0 \tag{3}$$

Eq.(3) is Laplace's equation – one of the most famous and extensively studied equations in mathematical physics. From Eq.(3), can be determined that inviscid, irrotational, incompressible flow (sometimes called potential flow) is governed by Laplace's equation.

4.2.2 Reynolds-Average Navier-Stokes Equation (RANSE)

The non-dimensional RANS equations for unsteady, three-dimensional incompressible flow can be written in Cartesian tensor notation as,

$$\frac{\partial U_i}{\partial t} + U_i \frac{\partial U_i}{\partial x^j} + \frac{\partial \overline{u_i u_j}}{\partial x^j} + \frac{\partial p}{\partial x^i} - \frac{1}{Re} \nabla^2 \mathrm{U_i} = 0 \tag{4}$$

where $U_i(i = 1,2,3) = (U, V, W)$ and $u_i(i = 1,2,3) = (u, v, w)$ are the Cartesian components of mean and fluctuating velocities, respectively, normalized by the reference velocity U_0, $x^i = (i = 1,2,3) = (X, Y, Z)$ is the dimensionless coordinates normalized by a characteristic length L, the Reynolds number is as follows:

$$R_e = \frac{U_0 L}{\nu} \tag{5}$$

ν is the kinematic viscosity, the barred quantities $-\overline{u_i u_j}$ are the Reynolds stresses normalized by U_0^2, and p is the pressure normalized by pU_0^2. If $-\overline{u_i u_j}$ are related to the corresponding mean rate of strain through an isotropic eddy viscosity, ν_t, i.e.

$$-\overline{u_i u_j} = \nu_t \left(\frac{\partial U_i}{\partial x^i} + \frac{\partial U_j}{\partial x^j} \right) - \frac{2}{3} \delta_{\mathrm{ij}} \mathrm{k} \tag{6}$$

Where $k = \overline{uu} + \overline{vv} + \overline{ww}/2$ is the turbulent kinetic energy, Equation (4) becomes

$$\frac{\partial U_i}{\partial t} + \left(U_j - \frac{\partial \nu_t}{\partial x^j} \right) \frac{\partial U_i}{\partial x^j} - \frac{\partial \nu_t}{\partial x^j} \frac{\partial U_j}{\partial x^i} + \frac{\partial p}{\partial x^i} \left(p - \frac{2}{3} \mathrm{k} \right) - \frac{1}{R_\emptyset} \nabla^2 \mathrm{U_i} = 0 \tag{7}$$

where $1/R_ø = 1/Re + \nu_t$, and $ø = U_i$ (i=1,2,3). Equations (5) and (7) can be solved for U_i and p when a suitable turbulence model is employed to calculate the eddy-viscosity distribution.

4.2.3 Grid Generation

The first step (and arguably the most important step) in CFD solution is generation of a grid that defines the cells on which flow variable (velocity, pressure, etc.) are calculated throughout the computational domain (Cengel and Cimbala, [6]). In this sub chapter discuss the two aspect that related to the grid generation on the CFD code as follow : a) Cubic Spline : use to interpolate between known data points; and b) Hess-smith panel method : collection of panels and expresses the flow field in body surface.

4.2.3.1 Cubic Spline

Cubic spline interpolation is a useful technique to interpolate between known data points due to its stable and smooth characteristics. The cubic spline has been utilized within the grid generation procedure to accurately model curves that may be found in engineering situations. This spline consists of weights attached to a flat surface at the points to be connected. A flexible strip is then bent across each of these weights, resulting in a pleasingly smooth curve. Consider a collection of known points $(x_0,$, $(x_1,$, ... $(x_{i-1}, y_i$, $(x_i$, $(x_{i+1}, y_i$, ... $(x_n,$. To interpolate between these data points using traditional cubic splines, a third degree polynomial is constructed between each point. The equation to the left of point $(x_i$, is indicated as with a value of $f_i($ at point . Similarly, the equation to the right of point $(x_i$, is indicated as with a value of $f_{i+1}($ at point .

If a set of data points is definitely a unique cubic polynomial can be defined between each set of points.

$$S(x) = \begin{cases} S_0(x) x\epsilon[x_0, x_1] \\ S_1(x) x\epsilon[x_1, x_2] \\ \cdot \\ \cdot \\ \cdot \\ S_{n-1} x\epsilon[x_{n-1}, x_n] \end{cases} \quad (8)$$

where is a third degree polynomial defined by

$$S_i(x) = a_i(x - x_i)^3 + b_i(x - x_i)^2 + c_i(x - x_i) + d_i \quad (9)$$

For $i = 1,2, \ldots, n$.

The first and second derivatives of these n - equations are fundamental to this process, and they are

$$S_i'(x) = 3a_i(x - x_i)^2 + 2b_i(x - x_i) + c_i \quad (10)$$

$$S_i''(x) = 6a_i(x - x_i) + 2b_i \quad (11)$$

for $i = 1,2, \ldots, n$.

4.2.3.2 Hess-smith Panel Method

The computer program based on the Hess-Smith panel method (HSPM) approximates the body surface by a collection of panels and expresses the flow field in terms of velocity potentials based on sources and vortices in the presence of an onset flow.

$$\emptyset = \emptyset_\infty + \emptyset_S + \emptyset_V \quad (12)$$

where, Ø is the total potential function and its three components are the potentials corresponding to the free stream, the source distribution, and the vortex distribution. These last two distributions have potentially locally varying strengths q and γ, where is an arc-length coordinate which spans the complete surface of the airfoil.

The potentials created by the distribution of sources/sinks and vortices are given by:

$$\emptyset_S = \int \frac{q(s)}{2\pi} \ln r ds \tag{13}$$

$$\emptyset_V = -\int \frac{\gamma(s)}{2\pi} \theta r ds \tag{14}$$

Combining Eqs. (12), (13) and (14)

$$\emptyset = +\int \frac{q(s)}{2\pi} \ln r ds - \int \frac{\gamma(s)}{2\pi} \theta r ds \tag{15}$$

The potential relation given above in Eq. (15) can then be evaluated by breaking the integral up into segments along each panel:

$$\emptyset = V_\infty (x \cos\alpha + y \sin\alpha) + \sum_{j=1_{panelj}}^{N} \int \left[\frac{q(s)}{2\pi} \ln r ds - \frac{\gamma}{2\pi} \right] dS \tag{16}$$

Since Eq. (16) involves integrations over each discrete panel on the surface of the airfoil, we must somehow parameterize the variation of source and vortex strength within each of the panels. Since the vortex strength was considered to be a constant, we only need worry about the source strength distribution within each panel. This is the major approximation of the panel method. However, you can see how the importance of this approximation should decrease as the number of panels, $N -$ (of course this will increase the cost of the computation considerably, so there are more efficient alternatives.)
Hess and Smith decided to take the simplest possible approximation, that is, to take the source strength to be constant on each of the panels

$$q(s) = q_i \text{ on panel } i, \qquad i = 1,2,\dots,N$$

Therefore, we have N + unknowns to solve for in our problem: the panel source strengths qi and the constant vortex strength . Consequently, we will need N + independent equations which can be obtained by formulating the flow tangency boundary condition at each of the panels, and by enforcing the Kutta condition discussed previously. The solution of the problem will require the inversion of a matrix of size $(N + 1) \times (N +$.

4.2.4 Froude number

The Froude number is named after the naval architect William Froude who studied the resistance of ships subjected to waves. The Froude number represents the ratio of inertia to gravitational forces, which generally is presented as:

$$\frac{\rho L^2 V^2}{\rho g L^2} = \frac{V^2}{gL} \tag{17}$$

Inertia and gravitational forces occur among others in the related topic open channel flow. The linear dimension L is significant for the flow pattern. Commonly the Froude number is expressed by taking the square root, to achieve a velocity of first power.

$$F_n = \frac{V}{\sqrt{gL}} \tag{18}$$

5. SIMULATION USING CFD

5.1 Round-shaped Model and Mesh Generation

The principal dimension of round-shaped FPSO is on the Table 1 below. The modeling of the round-shaped just uses diameter of the main hull and draft. The diameter of the pontoon is neglected. The Computational-Aid Design (CAD) use to model the round-shaped FPSO hull. Process of model round-shaped hull was started from the Maxsurf software. Model in the Maxsurf software then converts to CAD systems. Following Figure 2 shows the model of round-shaped FPSO in the CAD system.

Table 1 Principal Dimension of Round-shaped FPSO (Perwitasari, [20])

Description	Unit	Value
Diameter of Main Hull	m	90
Diameter of Pontoon	m	96.45
Draft	m	27
Mass	tonnes	182500
Radius of gyration in roll	m	28.5
Radius of gyration in pitch	m	28.5
Radius of gyration in yaw	m	42
Vertical center of gravity above keel, KG	m	22.85

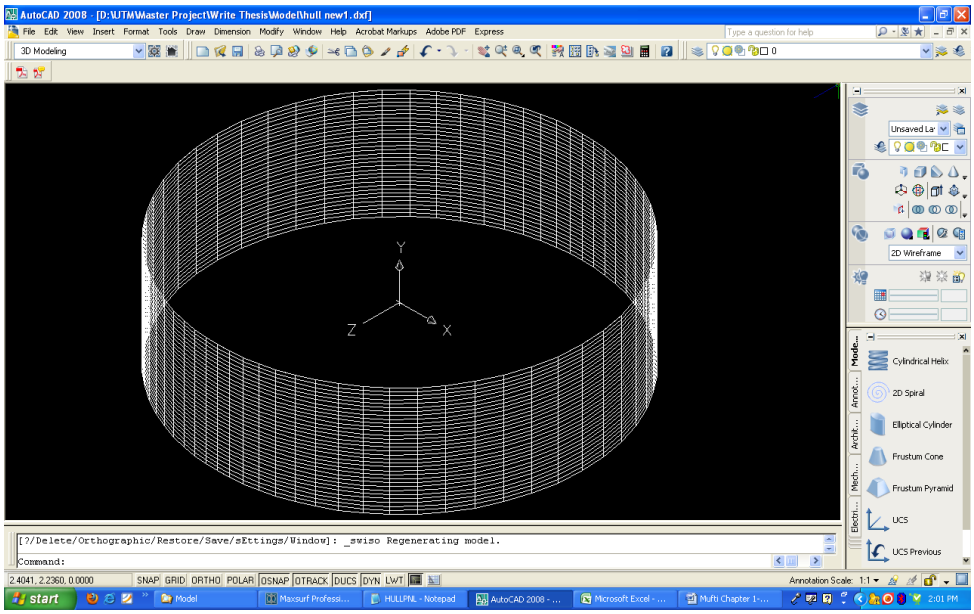

Fig. 2 Round-shaped FPSO Model in CAD systems.

Present studies using structured mesh with elliptic grid generation to solve the fluid flow. The configuration is 60 lines in longitude and 20 line in transversal. The dimension of elliptic is as follows:

a) radius of longitudinal is two times of length ship;
b) radius of transversal is one times of length ship; and
c) the origin of the coordinate from the center of the ellipse.

Following Figure 3 shows the mesh generation.

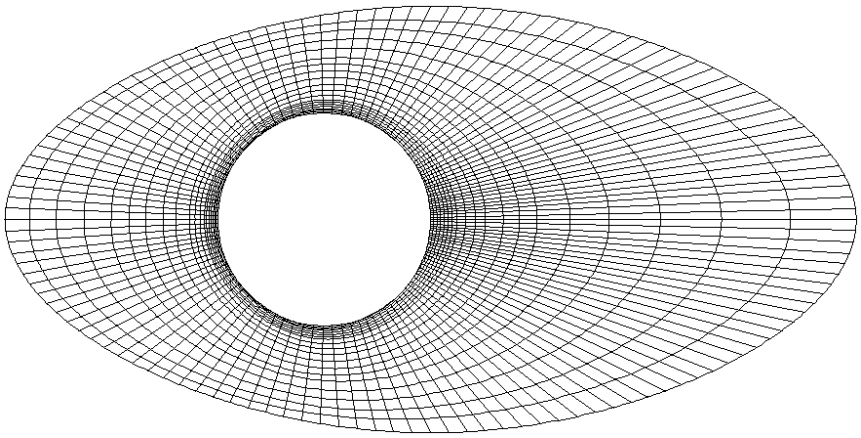

Fig. 3 Mesh Generation

There are several aspects that use for boundary condition in present study, as follow: a) Hull geometry modeled as a surface with three dimensional geometry; b) Fluid define as a free surface; and c) the direction of fluid from the head seas. The origin of coordinate in the boundary condition divided into two parts, local coordinate and global coordinate. Local coordinate is used for the hull geometry, located in the stem part of the hull. Global

coordinates is used to analyze fluid flow, located in the center of hull. Following Figure 4 shows the boundary condition that uses in the present study.

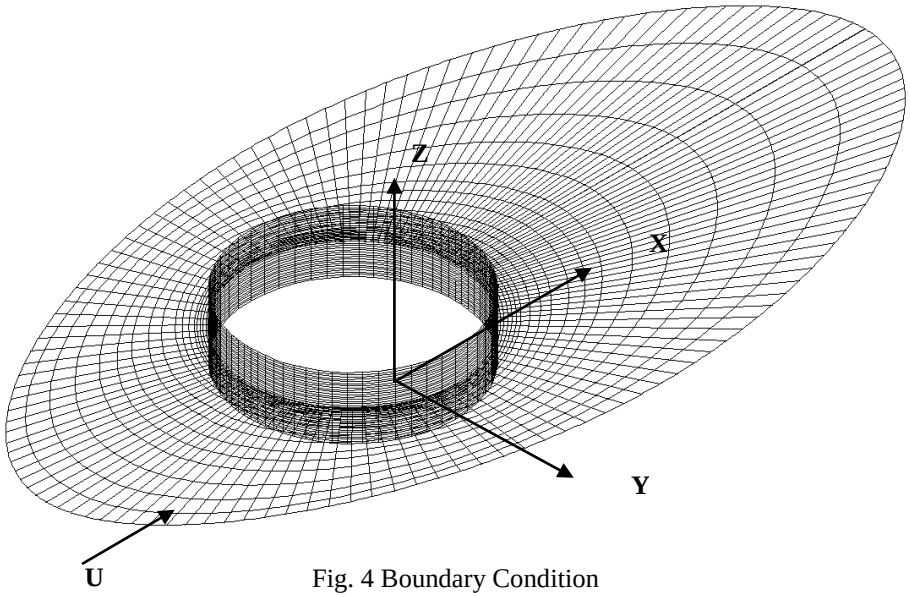

Fig. 4 Boundary Condition

5.2 Simulation Result

Results are presented in Figures 5.8–5.13 with different Fr. Fr value that used in the present study is 0.051, 0.102, 0.153, 0.204, 0.255, 0.306, 0.357, 0.408, 0.459 and 0.510. The discussions focus on comparisons with all the Fr. Present result is shown along the hull surface of the round-shaped model with x axis is X/(L/2) and y axis is Value/(L/2) respectively, where L is the length of round-shaped model and Value divided into three, Cp (Pressure), U (Axial velocity) and Z (Wave Elevation).

5.2.1 Pressure Distribution

For Fn = 0.051, 0.102, 0.153, 0.204, and 0.255, the pattern of the pressure distribution are same, with stem and stern part at positive region and middle part at a negative region (Figure 5). Pressure distribution at Fn = 0.255 given different value along the rounded-shape compare with the others. In the figure show that around the middle and stern part, the pressure distribution found higher than the others especially at the stern part ($0.6 < X/(L/2) < 1$).

For Fn = 0.306, 0.357, 0.408, 0.459 and 0.510, the pattern of the pressure distribution are same, with stem and middle part show slightly constant value and stern part shows changes value (Figure.6) . For all Fr the pressure distribution found lower value at the stem to middle part. The pressure distribution is founded changes with high value in the stern part of the rounded-shape hull for all Fr at $0.6 < X/(L/2) < 1$. With the changes in the stern part found in both Figure 5 and Figure 6, it indicates that this part given dynamic load at the rounded-shape hull. It is also indicated that the stern part is a critical part.

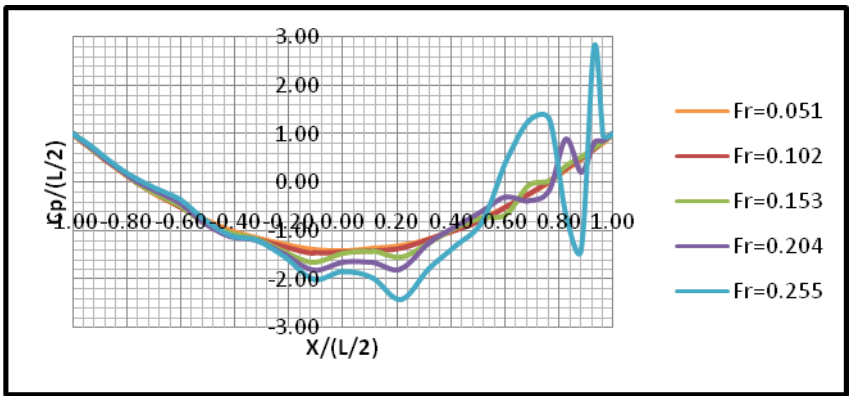

Fig. 5 Comparison of Pressure Profile with different Fn

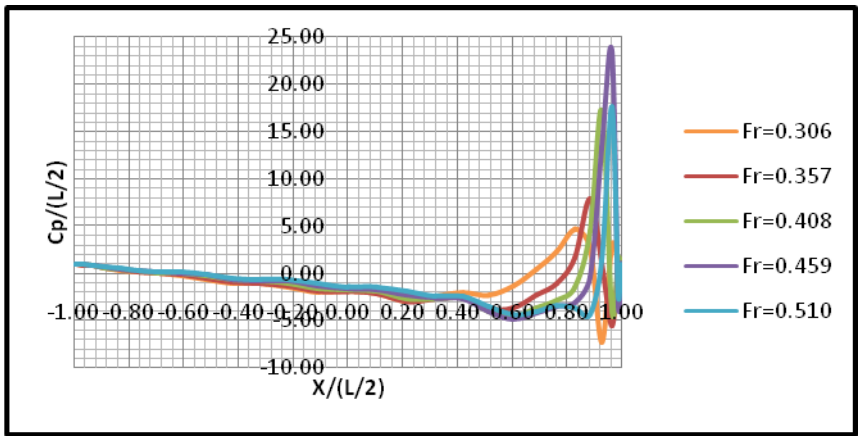

Fig. 6 Comparison of Pressure Profile with different Fn (Contd.)

5.2.2 Axial Velocity

For Fn = 0.051, 0.102, 0.153, 0.204, and 0.255, the pattern of the axial velocity are same, with middle part slightly higher than stem and stern part (Figure 7). Pressure distribution at Fn = 0.255 given different value along the rounded-shape compare with the others. In the figure show that around the middle and stern part, the axial velocity found consecutive higher and lower than the others especially at the stern part ($0.6 < X/(L/2) < 1$).

For Fn = 0.306, 0.357, 0.408, 0.459 and 0.510, the pattern of the pressure distribution are same, with stem and middle part show slightly a constant value and stern part show changes value (Figure 8). For all Fr the axial velocity is high value at the stem to middle part. The axial velocity is found changes with lower value in the stern part of the rounded-shape hull for all Fn at $0.6 < X/(L/2) < 1$. With the changes in the stern part found in both Figure 7 and Figure 8, it indicates that this part given dynamic load at the rounded-shape hull. It is also indicated that the stern part is a critical part.

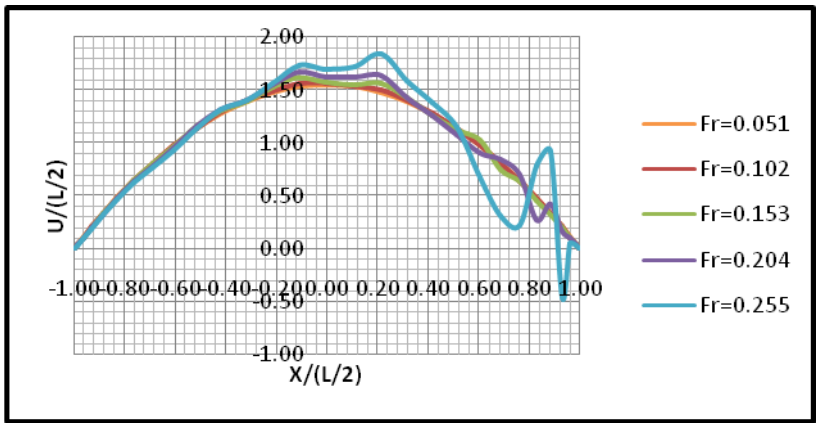

Fig. 7 Comparison of Axial Velocity with different Fr

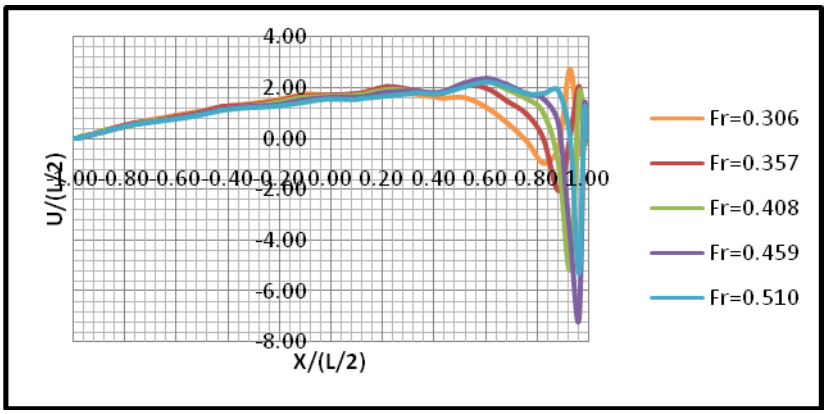

Fig. 8 Comparison of Axial Velocity with different Fn (Contd.)

5.2.3 Wave Elevation

For Fn = 0.051, 0.102, 0.153, 0.204, and 0.255, the pattern of the wave elevation are same, with middle part slightly higher than stem and stern part. At Fn = 0.051 and Fn = 0.102 show that the wave elevation along the rounded-shape are very small, slightly a constant value. Wave Elevation at Fr = 0.255 given different value along the rounded-shape compare with the others. In the figure show that around stern part ($0.6 < X/(L/2) < 1$), the wave elevation found higher than the others.

For Fn = 0.306, 0.357, 0.408, 0.459 and 0.510, the pattern of the wave elevation are same, with stem and middle part show slightly a constant value and stern part show changes value. For all Fr the wave elevation found low value at the stem to middle part. The wave elevation found changes with high value in the stern part of the rounded-shape hull for all Fr at $0.6 < X/(L/2) < 1$. With the changes in the stern part found in both Figure 9 and Figure 10, it indicates that this part given dynamic load at the rounded-shape hull. It is also indicated that the stern part is a critical part.

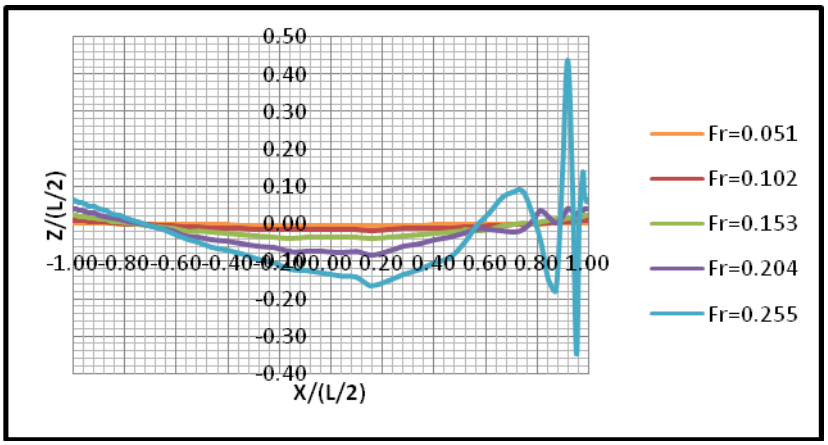

Fig. 9 Comparison of Wave Elevation with different Fn

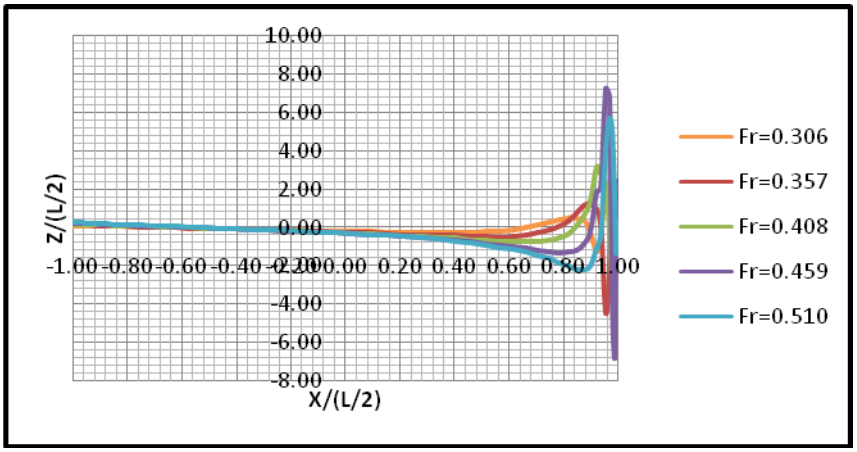

Fig. 10 Comparison of Wave Elevation with different Fn (Contd.)

6. CONCLUSIONS

Correspondingly with the increase in oil and gas exploration in deep ocean waters, there is growing interest to unlock and monetize these reserves with LNG FPSO (Liquified Natural Gas Floating Production Storage Offloading) facilities capable of liquefying and storing natural gas. Development of design concepts of the FPSO starts with a shape like a ship. Nowadays concept of FPSO is rounded-shape which is given much advantage than the ship-shape. From the previous study which is conducted by many researchers, it can conclude that study of the fluid flow around the hull is an important thing. Within the literature review, some of study has not conducted yet. Present study discusses an analysis of flow around a rounded-shape FPSO hull. The fluid flow characteristic around the rounded-shape LNG FPSO conducted using Computational Fluid Dynamics (CFD) based on the governing Reynolds Average Navier-Stokes (RANS) equations. Pressure distribution around the hull, axial velocity, and wave elevation value are simulated using CFD code with different Froude number. The obtained result found the critical part at stern ($0.6 < X/(L/2) < 1$). For future work the CFD code still need development to get the result with visualization, need to validate the simulation result with experimental data.

REFERENCES

1. Ahmed, Y.M., 2011, "Numerical simulation for the free surface flow around a complex ship hull form at different Froude numbers," Alexandria Engineering Journal, Vol. 50, pp. 229–235.

2. Ahmed, Y., Fonfach, J.M.A., and Soares, C. G., 2010, "Numerical Simulation for The Flow Around The Hull of The DTMB Model 5415 at Different Speeds," International Review of Mechanical Engineering, Vol. 4 (7), pp. 957-964.

3. Alexe, N., 2005, The Effects of The Dimensions, "The Shape and The Speed of The Ship on The Pressure Distributions in Surrounding Sea Water," Oceans 2005 – Europe, Vol. 2, pp. 1347-1350.

4. Arslan, T., Pettersen, B. and Andersson, H.I., 2011, "Calculation of the Flow Around Two Interacting Ships," Computational Methods in Marine Engineering IV, L.Eça, E. Oñate, J. García, T. Kvamsdal and P. Bergan (Eds.), pp. 254-265.

5. BrogliaR.,Zaghi, S. and Mascio, A. D., 2011, "Numerical Simulation of Interference Effects for A High-Speed Catamaran," Journal of Marine Science and Technology, Vol. 16, pp. 254–269.

6. Cengel, Y.A. and Cimbala, J. M., 2006, "Fluid Mechanic: Fundamental and Applications," New York : McGraw-Hill.

7. Ciortan, C. et al, 2005, "Calculation of the Flow Around Ship Hulls Using a Parallel CFD Code," Parallel Computational Fluid Dynamics - Multidisciplinary Applications, G. Winter, A. Ecer, J. Periaux, N. Satofuka and P. Fox (Editors). pp. 215-221.

8. Ciortan, C., Soares, C.G., and Wanderley, J., 2008, "Free Surface Flow Around Ship Hulls Using an Interface-Capturing Method," Proceedings of the International Conference on Offshore Mechanics and Arctic Engineering - OMAE, Vol. 5, pp. 979-986.

9. Ciortan, C.,Wanderley, J., and Soares,C. G., 2007, "Turbulent Free-Surface Flow Around a Wigley Hull Using The Slightly Compressible Flow Formulation," Journal of Ocean Engineering, Vol.34, pp. 1383–1392.

10. Ciortan,C., Wanderley,J.B.V., and Soares, C. G., 2012, "Free Surface Flow Around a Ship Model Using an Interface-Capturing Method," Journal of Ocean Engineering, Vol. 44, pp 57–67.

11. Deng, G.B., Queutey, P., and Visonneau, M., 2006, "Turbulent Flow Prediction Around Appended Hulls," Journal of Hydrodynamics, Ser. B, Vol. 18 (3), pp. 225-231.

12. Jaswar et al, 2011, "An integrated CFD simulation tool in naval architecture and offshore (NAO) engineering," The 4th International Meeting of Advances in Thermo fluids (IMAT 2011), 3–4 October, Melaka, Malaysia, AIP Conf. Proc. 1440, pp. 1175-1181.

13. Jones, D.A. and Clarke, D.B, 2010, Fluent Code Simulation of Flow around a Naval Hull: The DTMB 5415," Maritime Platforms Division, Defence Science and Technology Organisation, Victoria, Australia.

14. Kim, S.-E., 2003, "A Numerical Investigation of Three-Dimensional Turbulent Shear Flow around a Ship Hull at Straight Maneuver. Proceedings of the ASME Fluids Engineering Division Summer Meeting, Vol. 1, pp. 865-870.

15. Kim, W. -J. , Kim, D.-H., Van Suak, H, 2002, "Computational study on turbulent flows around modern tanker hull forms," International Journal for Numerical Methods in Fluids, Vol. 38 (4), pp. 377-406.

16. Kinnas, S. A., Yu, Y. H., and Vinayan, V., 2006, "Prediction of Flows around FPSO Hull Sections in Roll Using an Unsteady Navier-Stokes Solver," Proceedings of The Sixteenth International Offshore and Polar Engineering Conference, pp. 384-393.

17. Lamport, W. B. and Josefsson, P.M., 2008, "The Next Generation Of Round Fit-For-Purpose Hull Form FPSOS Offers Advantages Over Traditional Ship-Shaped Hull Forms," DeepGulf Conference, December 9-11, New Orleans, Louisiana, USA.

18. Lungu, A., 2007, "Numerical simulation of the free-surface turbulent flow around a VLCC ship hull," AIP Conference Proceedings, Vol. 936, pp. 647-650.

19. Paik, J.K., Thayamballi, A.K., (2007), "Ship-Shaped Offshore Installations: Design, Building, and Operation," Cambridge University Press, Cambridge, UK.

20. Perwitasari, R. N., 2010, "Hydrodynamic Interaction And Mooring Analysis For Offloading Between FPSO And LNG Shuttle Tanker," Master Thesis, Department of Marine Technology, NTNU.

21. Schweighofer, J. et al., 2005, "Viscous-Flow Computations of Two Existing Vessels ot Model- and Full-Scale Ship Reynolds Numbers: A Study Carried Out Within The European Union Project, EFFORT.," International Conference on Computational Methods in Marine Engineering MARINE 2005, P. Bergan, J. Garc´ıa, E. O˜nate and T. Kvamsdal (Editors), CIMNE, Barcelona.

22. Sevan Marine ASA., 2009, FPSO International : Felix Conference Center, March 4, 2009, Oslo, Norway. http://www.intsok.com/style/downloads/Sevan--PDF-Presentation-FPSO-Co.pdf .Access Date : May, 8th 2012.

23. Srinivasan et al, 2008, "Design of Non-Ship-Shape FPSO for Sakhalin-V Deepwater," SPE Russion Oil and Gas Technical Conference and Exhibition, 28-30 October, Moscow, Russia.

24. SSP Offshore Inc., 2010, "The Next Generation Round "Fit-for- Purpose" Hull Form FPSOs/FDPSOs Offers Advantages over Traditional Ship-Shaped Hull Forms," World FPSO Conversion & Floating LNG Facilities Conference, 22-23 February, Kuala Lumpur, Malaysia.

25. Tahara, Y. et al., 2008, "Development and Demonstration of CAD-CFD-Optimizer Integrated Simulation-Based Design Framework by Using High-Fidelity Viscous Free-Surface RANS Equation Solver," Journal of the Japan Society of Naval Architects and Ocean Engineers, Vol. 7, pp. 171-184.

26. Tahara, Y. et al., 2006, "RANS Simulation of a Container Ship Using a Single-Phase Level-Set Method with Overset Grids and The Prognosis for Extension to a Self-Propulsion Simulator," Journal of Marine Science Technology, Vol. 11, pp. 209–228.

27. Visonneau, M., 2005, "A Step towards the Numerical Simulation of Viscous Flows Around Ships at Full Scale - Recent Achievements Within The European Union Project EFFORT, RINA," Royal Institution of Naval Architects International Conference - Marine CFD 2005: 4th International Conference on Marine Hydrodynamics, pp. 1-8.

28. Wackers,J. et al., 2011, "Free-Surface Viscous Flow Solution Methods for Ship Hydrodynamics," Archive of Computational Methods in Engineering, Vol. 18, pp. 1–41.

29. Wan, D.-C., Shen, Z.-R., and Ma, J., 2010, "Numerical simulations of viscous flows around surface ship by level set method," Journal of Hydrodynamic, Vol. 22 (5), pp. 271-277.

30. Wang, H.-M, Zou, Z.-J., and Tian X.-M., 2009, "Computation of the Viscous Hydrodynamic Forces on a KVLCC2 Model Moving Obliquely in Shallow Water," Journal of Shanghai Jiaotong University (Science), Vol. 14 (2), pp. 241−244.

31. Wang, J.-B. et al., 2010, "Numerical Simulation of Viscous Wake Field and Resistance Prediction Around Slow-Full Ships," Chinese Journal of Hydrodynamics Ser. A., Vol. 25 (5), pp. 648-654.

32. Wang, T. Y., Zhang, J., and Liu, J. K., 2012, "Concept Design of a New Non-Ship-Shaped FPSO," Applied Mechanics and Materials, Vol. 170-173, pp. 2222-2227.

33. Hu, Weihua, 2012, "Numerical Simulation of the Viscous Flow around High-speed Ship Hull Considering the Free Surface," Journal of Applied Mechanics and Materials. Vol. 101-102, pp. 966-969.

34. Zhang, Z.-R., Zhao, F., and Li, B.-Q., 2002, "Numerical Calculation of Viscous Free-Surface Flow about Ship Hull," Journal of Ship Mechanics, Vol. 6 (6), pp. 10-17.

35. Zhao, F., and Zhang, Z.-R., 2003, "Numerical Simulation of Viscous Flow Around Ship Model DTMB 5415," Proceeding of the 2003 17th National Conference on Hydrodynamics and the 6th National Congress on Hydrodynamics 2003, pp. 345-351.

36. Zhao, F., Zhu, S.-P., and Zhang, Z.-R., 2005, "Numerical Experiments of A Benchmark Hull Based on a Turbulent Free-Surface Flow Model," CMES - Computer Modeling in Engineering and Sciences, Vol. 9 (3), pp. 273-285.

37. Zwart, P. J.,et al., 2008, "Simulation of Unsteady Free-Surface Flow Around a Ship Hull Using a Fully Coupled Multi-Phase Flow Method," Journal of Marine Science and Technology, Vol. 13, pp 346–355.

38. E.Afrizal, F.M. Mufti, C.L.Siow, Jaswar, 2013, "Study of Fluid Flow Characteristic around Rounded-Shape FPSO Using RANS Method," The 8th International Conference On Numerical Analysis In Engineering, Pekanbaru, Indonesia.